Journal of Ceramic Processing Research. Vol. 20, No. 6, pp. 643~648 (2019)
(Received 19 July 2019, Received in revised form 8 October 2019, Accepted 20 October 2019)
https://doi.org/10.36410/jcpr.2019.20.6.643

J O U R N A L O F
Ceramic Processing Research

Roles of talc-illite on phase transformation, vitrification and physical properties of a triaxial porcelain body

Suthee Wattanasiriwech[a,b] and Darunee Wattanasiriwech[a,b,*]
[a]*Center of Innovative Materials for Sustainability, School of Science, Mae Fah Luang University, Thailand*
[b]*Circular Economy for Waste-free Thailand Research Group, Mae Fah Luang University, Thailand*

Flux forming additives have played an important role of energy reduction in the ceramic industry for centuries. Though there are available fluxing materials in the market, attempts of searching for new flux systems have still been extensively done. This paper presents the use of a combined flux system and its roles on phase transformation and physical properties of a triaxial porcelain body. Illite was used as the primary flux in the main recipe while talc, the supplementary flux, was added at 0, 3, 5 weight %. In pure form, talc dissociated into enstatite around 900 ºC but when mixed in the recipe, phase changes of talc differed. Talc and illite disappeared around 1,000 ºC. Around 1,200-1,300 ºC, indialite and pyrophillite appeared only on the body with talc addition. Early densification could be observed when talc was present, suggesting that talc also played an important role in vitrification. The body with 3% talc showed the greatest firing shrinkage and flexural strength but lowest water absorption after firing at 1,200 ºC, which was ~50 ºC lower than the body without talc. Further increasing of talc content to 5% resulted in an adverse effect of these properties.

Key words: Triaxial porcelain, Illite, Talc, Phase transformation, Vitrification.

Introduction

Porcelains are vitreous ceramic whitewares which are used extensively in table wares, dental prosthetics, and decorative wares. With the room temperature resistivity between 10^{12}-10^{14} Ω, porcelain ceramics are extensively used as an insulating material [1]. Porcelains typically have a triaxial formulation comprising of clay-feldspar-quartz as the main ingredients. Quartz is partially added to reduce pyroplastic deformation [2]. Due to the high firing temperature (>1,200 ºC for soft porcelain and 1,400 ºC for hard porcelain), flux-forming additives were generally employed in order to reduce the energy consumption without compromising productivity and product [3-6]. Some of the reported works are exemplified here. Das compared densification behavior of K-and Na-feldspar-containing porcelain bodies and found that Na-feldspar containing body exhibited maximum densification rate at 1,171 ºC compared to 1,195 ºC for the K-feldspar containing body [7]. The Na-feldspar containing body achieved higher density, lower water absorption and highest flexural strength at 1,200 ºC. Dana et al. have reported the enhancement in densification and strength of triaxial porcelain when B.F. slag was used in substitution of potash feldspar [8]. The addition of slag resulted in the diminishment of quartz and mullite needles but development of anorthite phase ($CaO{\cdot}Al_2O_3{\cdot}2SiO_2$). Bragança and Berman showed that the glass-powdered porcelain in which feldspar was replaced by recycled soda-lime glass sintered at 100 ºC lower than the traditional porcelain [9]. However, when fired at the proper temperature, traditional porcelain exhibited higher modulus of rupture due to the presence of secondary mullite crystals. Combined flux system was typically used along with the aids of muscovite mineral [10]. Pyroplastic deformation, which is related to properties of liquid phases formed during firing, was found to be influenced by ratio of the key ions used in the formula. It was reported that that a definite combination at SiO_2/Al_2O_3 ratio of 5 and Na_2O/K_2O ratio of 4 gave the lowest pyroplastic deformation in the porcelain body formulations [11].

Some of the reported literatures proposed an alternative method in energy consumption reduction such as direct sintering method whose total processing time was reduced by a factor of 50% and the sintering temperature was decreased from 1,200 ºC to 1,175 ºC [12]. In this scenario, sample was delivered directly to the furnace pre-set at the sintering temperatures. The samples were held for 15 min before cooling down to 700 ºC at a rate of 30 ºC/min and followed by cooling to room temperature. The use of microwave sintering was reported to reduce sintering temperature by ~75ºC and reduce dwell time from 15 min to 5 min while retaining comparable physical properties [13].

As previously discussed, the irreversible thermal expansion of ceramic bodies containing ball clay started

*Corresponding author:
Tel : +6653916263
Fax: +6653916776
E-mail: darunee@mfu.ac.th

around 900 ºC [14]. Most ball clay contains illite, which is a mica- type mineral with its high potassium content in its structure, and thus fusibility. The structure of illite is composed of two tetrahedral sheets sandwiched to an octahedral sheet to form a 2:1 layer phyllosilicate. Illite serves as an excellent flux because of its small particle size and being a part of body matrix. The body porosity was, thus, reduced by the onset of melting and the bodies began to shrink at a temperature as low as 900 ºC [14]. This result was in good agreement with a study by Aras [15], who used illite in substitution of kaolin. It was shown that the high K content in illite caused a large amount of liquids and the reduction of mullite formation temperature. When illitic clay was fired, illite structure first collapsed around 900-950 ºC resulting in liquid phase formation [16, 17]. Another study using an in-situ high temperature X-ray diffraction showed that transition from illite phase to dehydroxylated phase started around 525 ºC in static air and higher at about 550 ºC in vacuum. Phase transformation from dehydroxylated to mullite occurred at above 1,100 ºC [18]. It was also pointed out that transformation could be affected by sample's properties such as particle size, crystallinity, and vacant type [19]. Illite was reported to gradually diminish at 600 ºC before completely disappearing at 800 ºC upon firing [19]. Our previous attempt to use illite as the primary flux in place of a potash feldspar in a triaxial porcelain body was achieved and the firing temperature could be lowered up to 100 ºC [20].

Talc is a hydrated magnesium sheet silicate with the chemical formula $Mg_3Si_4O_{10}(OH)_2$. Talc has a 2:1 structure with an octahedral brucite sandwiched between two tetrahedral silicate layers [21]. Talc is typically used as a filler in composite materials to decrease the production costs while improving the physical and chemical properties and also providing new functionalities [22]. From literatures, talc progressively lost its hydroxyl groups at above 900 ºC and re-crystallized into different forms of enstatite (anhydrous magnesium silicate) above 1,050 ºC before melting at 1,500 ºC [23]. The use of talc with other fluxes e.g. nepheline syenite has been reported [24]. Appropriate amount of talc added to the stoneware body was reported to give optimum properties and decrease sintering temperature [25]. When feldspar was partly replaced by talc, the body fired at high temperature contained more liquid of lower viscosity than the standard body containing only feldspar flux [26].

In this study, our further attempt to reduce the firing temperature with the aids of talc in the body containing illite as the primary flux was performed. Phase changes and physical properties were determined and discussed here.

Experiments

China clay whose main minerals were halloysite and kaolinite was received from Ranong province, Thailand. Quartz and talc ($Mg_3Si_4O_{10}(OH)_2$) were purchased from a domestic commercial supplier. The illite mineral ($K_yAl_4Si_{8-y}Al_yO_{20}(OH)_4$) where y = 1-1.5, Green shale) was received from Ward's Natural Science, Rochester, New York, USA. Analysis of illite and china clay was previously reported [20]. Analysis of talc was assessed using standard protocols, X-ray diffraction (XRD), scanning electron microscopy (SEM), and size analysis using laser diffraction. The lateral size (a) of plate-like talc particle was analyzed based on the method described by Pérez-Maqueda et al. as shown in Eq. (1) [27]:

$$a = \sqrt{\frac{\frac{4}{3}\pi\left(\frac{esd}{2}\right)^3}{d_{001}}} \tag{1}$$

d_{001} (4.67 nm or 4.67×10^{-9} m) was determined from the broadening of XRD peak. *esd* is the equivalent spherical diameter (m) which can be calculated from Eq. (2) as follows;

$$esd = \frac{6}{\rho \cdot S} \tag{2}$$

where S is the specific surface area (6.02 $m^2 \cdot g^{-1}$) determined using the BET technique and ρ is the density (2.8 $kg \cdot m^{-3}$).

The body recipe contained 50 weight % china clay, 25 weight % quartz and 25 weight % illite. Talc (0, 3, 5 weight %) was finally added and the samples were denoted as *IT0*, *IT3* and *IT5* respectively. Details of experiments were also previously addressed [20]. Summary of the experiment is given shortly here. The starting materials were mixed, ground using a ball milling technique and sieved through a 325-mesh sieve prior to drying in an oven overnight. The dried clay was then pressed at a compaction pressure of 50 MPa into a rectangular bar with the dimensions of 5 mm × 5 mm × 60 mm. Each set of the test samples was heated in the range of 900-1,300 ºC in air atmosphere. Water absorption of the fired samples was examined based on the Archimedes' principle with the details of experiment reported in ref [28]. The flexural strength was measured using a Universal Testing Machine (Instron 2000, UK) by the three-point bending technique. For all measurements, the support span of 80 mm and the crosshead speed of 5 mm/min were selected. The flexural strength was measured using the formulae $\sigma = 3/2\ [(FL)/bd^2]$, where is the flexural strength, F is the load at the fracture point (N), L is the span length; b and d are the width and thickness of the specimens respectively. These values, which were averaged from five samples, were plotted as a function of firing temperature. Phase analysis was observed using an X-ray diffraction (XRD) technique

equipped with the software X'pert High Score Plus (X'pert Pro MPD, Philips, Netherlands). Microstructural development of the fired bars was examined with scanning electron microscope (SEM: LEO 1450 VP). The fired test bars were etched with 4% hydrofluoric acid (HF) before the microscopical examination.

Results and Discussion

Analysis of phase changes, chemical contents and particle size of clay and illite were reported elsewhere [20] so only analysis of talc is addressed in this paper. Lateral size of the talc was calculated according to Eq. (1) was 2.19 mm. Morphological observation using an SEM of the talc used in this study is shown in Fig. 1. X-ray diffraction (XRD) analysis (Fig. 2) shows that talc mainly contained talc mineral with a small amount of quartz and magnesite ($MgCO_3$) as well as a small trace of dolomite ($CaCO_3 \cdot MgCO_3$). Upon firing to 800 ºC, talc reflections started to diminish. Reflections of enstatite ($MgSiO_3$) started to appear around 900 ºC. This result was in good agreement with the report by Sabouang et al. [29].

XRD spectra of the fired sample bars are displayed in Fig. 3. Only those with 5% talc are shown since the samples with less percentage of talc had relatively similar reactions upon firing but with lesser extensity of the phase compositions due to the lesser content of talc. At 900 ºC, reflections belonging to quartz, illite and talc existed. It was noted that the reflections belonging to enstatite, which appeared when pure talc was fired, were not observed in the spectra. At 1,000 ºC, talc and illite reflections disappeared while mullite started to emerge and got stronger in intensity with the increase of firing temperatures. Primary mullite content was reported to slightly increase with increased sintering temperature through transformation mullitization process of kaolinite [28]. At 1,200-1,300 ºC, two types of other aluminosilicate minerals, indialite and pyrophyllite, appeared. Indialite ($Mg_2Al_4Si_5O_{18}$), with a chemical formula similar to cordierite, had a hexagonal structure so it was once thought to be cordierite appeared at these temperatures. However, the work done by Miyashiro showed that cordierite had a triplet around 29-30 º2θ, while indialite only showed a single reflection at this region [30]. Some recent literatures, however, stated that indialite is a high temperature form of cordierite [31, 32]. The reflection at 9.5 º2θ could be indexed as pyrophyllite ($Al_2Si_4O_4(OH)_2$) or talc (X'pert High Score Plus: reference number 00-003-0170 and 00-003-0881 respectively) due to the close peak positions of these two compounds at this angle. Pyrophyllite is a 2:1 clay mineral without interlayer cation similar to talc [33]. If this reflection

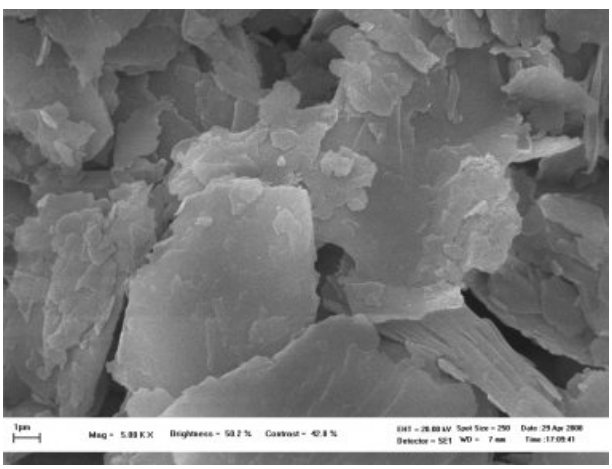

Fig. 1. SEM micrograph of talc particles revealing their platy shape.

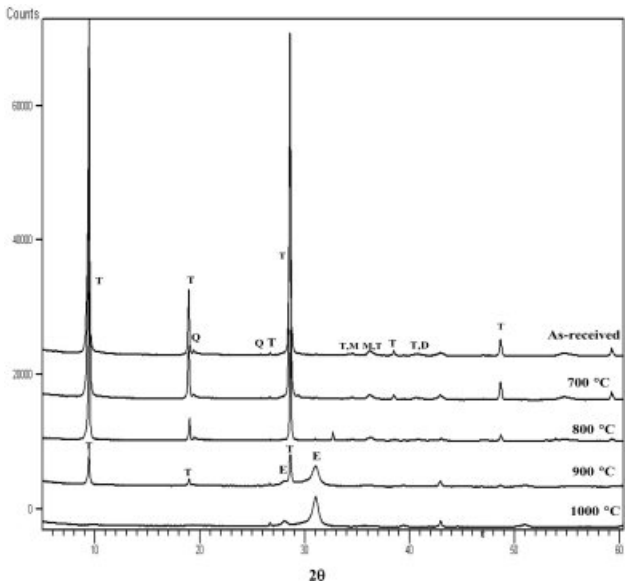

Fig. 2. XRD spectra for talc fired at various temperatures (T: talc, Q: quartz: M: magnesite, D: dolomite).

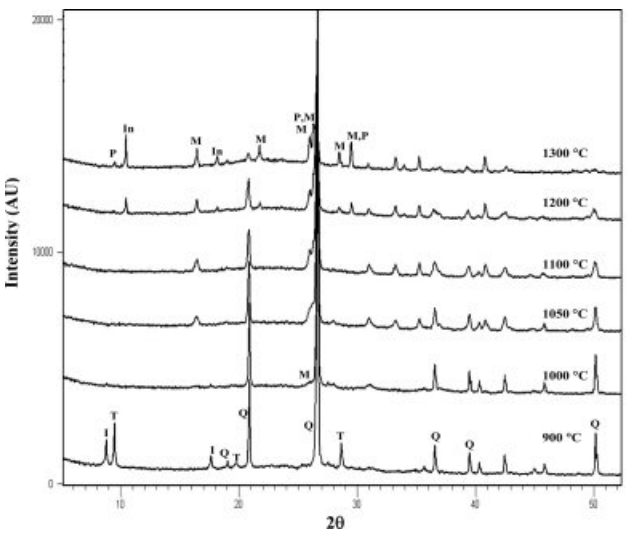

Fig. 3. XRD patterns spectra for the samples with 5% talc addition fired at different temperatures (M: mullite, Q: Quartz, I: Illite, In: Indialite, P: Pyrophyllite).

truly belonged to talc, it would be puzzling as to how it reappeared. Re-examination on another sample gave the same result, suggesting that this observation was reliable. Neither enstatite nor dehydrated talc, which appeared in the heat-treated pure talc sample, was observed in this set of samples. It is noted that indialite and pyrophyllite (or talc) reflections were not observed in the *IT0* samples.

Key physical properties of the samples such as firing shrinkage and water absorption as well as mechanical properties are shown in Fig. 4. The *IT0* samples showed the greatest shrinkage at 1250 ºC while the *IT3* and *IT5* samples showed the greatest shrinkage at around 1,200-1,250 ºC and 1,200 ºC respectively (Fig. 4(a)). All the samples showed expansion due to expansion of

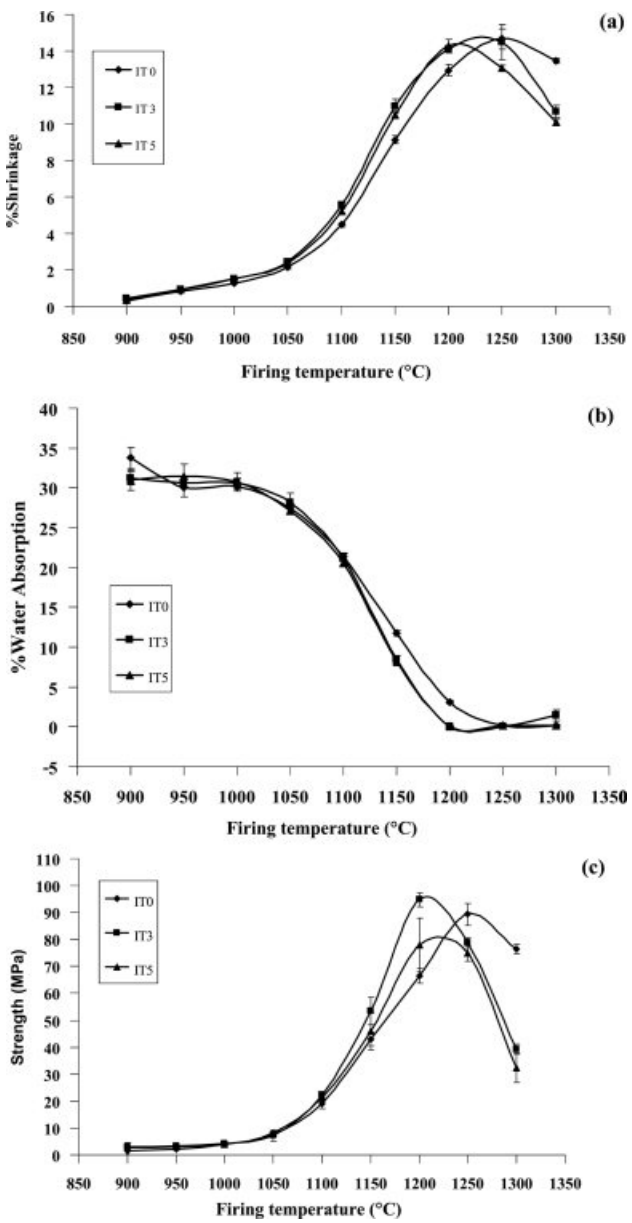

Fig. 4. Variation of (a) firing shrinkage (b) water absorption and (c) flexural strength as a function of firing temperatures of the samples with different talc contents.

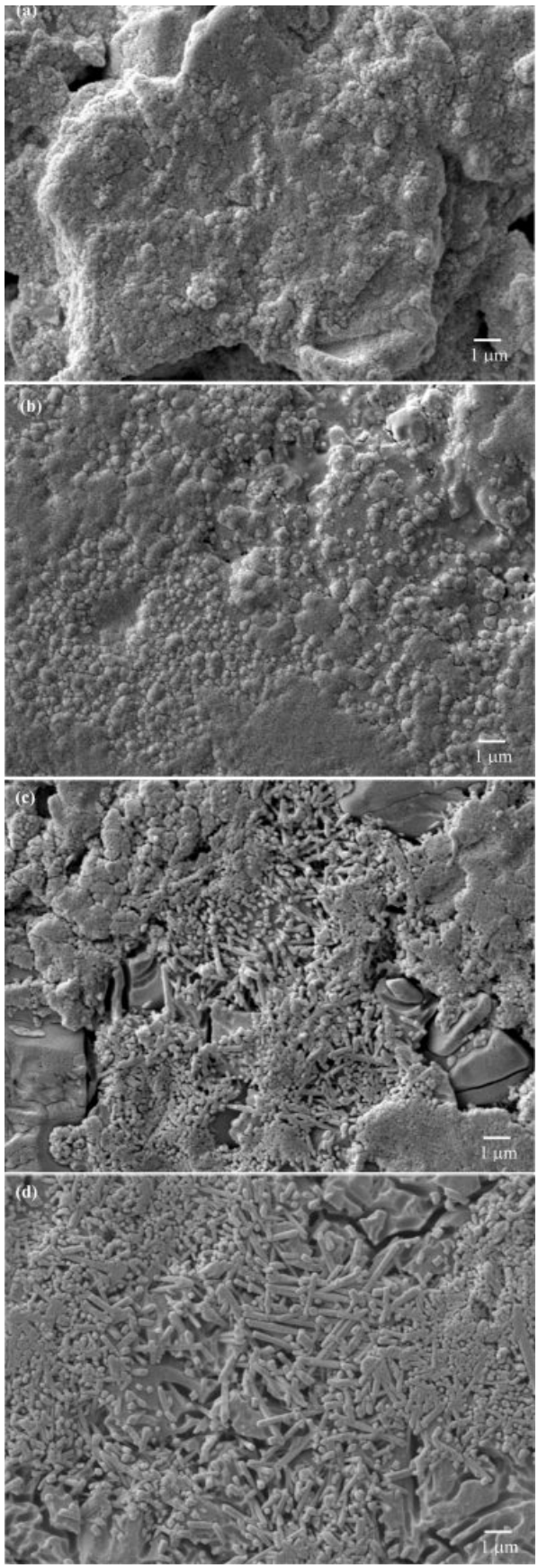

Fig. 5. Microstructural development of the body with 3% talc addition after firing at (a) 1,000 ºC, (b) 1,100 ºC, (c) 1,200 ºC and (d) 1,300 ºC.

trapped gas (bloating) after reaching the greatest shrinkage. Trapped air in a ceramic body could be caused by arise due to over firing, too rapid firing, or the increase in the content of volatile materials such as manganese oxide and iron ochre [34]. In our present study, it was believed that over firing was the reason for bloating as also suggested by the finding by López and Rodríguez [35]. Water absorption was also smallest when the shrinkage was highest but slightly increased when bloating occurred (Fig. 4(b)). Flexural strength for the *IT0* sample was greatest after firing at 1,250 ºC. Improvement of strength was found in the *IT3* sample with the reduction of optimum temperature to 1,200 ºC. Deterioration of the strength was observed in the *IT5* sample primarily due to bloating (Fig. 4(c)).

SEM micrographs for the specimens with 3% talc heat treated at 1,000-1,300 ºC are shown in Fig. 5. At 1,000 ºC. The surface was fully covered with nanocrystals and early stage of densification was also observed (Fig. 5(a)). In the sample with 0% talc, these crystals were suggested to be mullite formed by decomposition of illite because primary mullite was not normally observable at this temperature [20]. Increasing the firing temperature to 1,100 ºC, the nanocrystalline mullite did not appreciably grow while progressive densification could be observed (Fig. 5(b)). At 1,200 ºC, elongated mullite of up to 1 mm long (as estimated using the SEM scale) appeared while cubical mullite was still generally observed (Fig. 5(c)). It was noted that this elongated mullite was laterally larger than needle shaped mullite typically observed in a standard porcelain body. In a typical porcelain body where feldspar was used as a single flux, the outer rim of the feldspar relict showed a clear boundary to the clay relict. Needle shaped-mullite crystals originated on this boundary and grew into the liquid pool relict. In this experiment, however, such boundary and liquid pool relict were not so visible due to the different source and location of the liquid former being used. Morphology of the secondary mullite was thus different as a result of the mentioned reason. At 1,300 ºC (Fig. 5(d)), both mullite types grew in size and covered almost all the areas.

Conclusion

This paper presents the use of talc as in auxiliary flux to illite in a triaxial body. When it was incorporated in the recipe, phase transformation up on firing of talc was found to be different from that found in the pure form. his research showed that talc could be used as a supplemental flux in the body containing illite as a primary flux with improved body properties and reduction of the peak firing temperature. However, the amount of talc contents should not exceed 3 weight % addition otherwise deterioration of the properties especially flexural strength would be obtained due to bloating of the body.

Acknowledgement

The authors would like to thank Mae Fah Luang University, Thailand for the financial and laboratory support.

References

1. A.N.N. Dowuona, A. Yaya, E. Nyankson, J.K. Efavi, L.N.W. Damoah, D. Dodoo-Arhin, V. Apalangya, E. Annan, E.K. Tiburu, B. Onwona-Agyeman, and B. Tomiczek, J. Ceram. Process. Res. 19[2] (2018) 95-100.
2. J. Choi, K. Hwang, U. Kim, K. Ryu, K. Shim, and S. Kang, J. Cearmic Process. Res. 20[4] (2019) 424-430.
3. R.H. and A.B.A. S. Natrah, Int. J. Autom. Mech. Eng. 16[2] (2019) 6649-6659.
4. D.U. Tulyaganov, S. Agathopoulos, H.R. Fernandes, and J.M.F. Ferreira, J. Eur. Ceram. Soc. 26[7] (2006) 1131-1139.
5. Y.U. and S.Ö.A. Karaa, K. Kayacic, and A.S. Küçükerc, V. Bozkurtd, Ind. Ceram. 29[2] (2009) 71-81.
6. L.A. Carús, F. de Souza, and S.R. Bragança, ISRN Ceram. 2012 (2012) 1-7.
7. S.K. Das and K. Dana, Thermochim. Acta 406[1-2] (2003) 199-206.
8. K. Dana and S.K. Das, J. Eur. Ceram. Soc. 24[15-16] (2004) 3833-3839.
9. S.R. Bragança and C.P. Bergmann, J. Eur. Ceram. Soc. 24[8] (2004) 2383-2388.
10. P. Lima, A. Zocca, W. Acchar, and J. Günster, J. Eur. Ceram. Soc. 38[9] (2018) 3395-3400.
11. D.Y. Tunçel, M.K. Kara, and E. Özel, IOP Conf. Ser. Mater. Sci. Eng. 18[22] (2011) 222025.
12. W. Lerdprom, R.K. Chinnam, D.D. Jayaseelan, and W.E. Lee, J. Eur. Ceram. Soc. 36[16] (2016) 4319-4325.
13. W. Lerdprom, E. Zapata-Solvas, D.D. Jayaseelan, A. Borrell, M.D. Salvador, and W.E. Lee, Ceram. Int. 43[16] (2017) 13765-13771.
14. D. Wattanasiriwech, K. Srijan, and S. Wattanasiriwech, Appl. Clay Sci. 43[1] (2009) 57-62.
15. A. Aras, Appl. Clay Sci. 24[3-4] (2004) 257-269.
16. R. E. Grim and W. F. Bradley, J. Am. Ceram. Soc. 23[8] (1940) 242-248.
17. A. Khalfaoui, S. Kacim, and M. Hajjaji, J. Eur. Ceram. Soc. 26[1-2] (2006) 161-167.
18. G. Wang, H. Wang, and N. Zhang, Appl. Clay Sci. 146 (2017) 254-263.
19. S. Boussen, D. Sghaier, F. Chaabani, B. Jamoussi, and A. Bennour, Appl. Clay Sci. 123 (2016) 210-221.
20. D. Wattanasiriwech and S. Wattanasiriwech, J. Eur. Ceram. Soc. 31[8] (2011) 1371-1376.
21. S. Farrokhpay, B. Ndlovu, and D. Bradshaw, Appl. Clay Sci. 160 (2018) 270-275.
22. A. Dumas, F. Martin, E. Ferrage, P. Micoud, C. Le Roux, and S. Petit, Appl. Clay Sci. 85 (2013) 8-18.
23. M. Hojamberdiev, P. Arifov, K. Tadjiev, and Y. Xu, Min. Sci. Technol. 20[3] (2010) 415-420.
24. L. Esposito, A. Salem, A. Tucci, A. Gualtieri, and S.H. Jazayeri, Ceram. Int. 31[2] (2005) 233-240.
25. M.U. Taskiran, N. Demirkol, and A. Capoglu, J. Eur. Ceram. Soc. 25[4] (2005) 293-300.
26. M. Dondi, V. Biasini, G. Guarini, M. Raimondo, A. Argnani, and S. Di Primio, Key Eng. Mater. 206-213[II] (2001) 1795-1798.

27. L.A. Pérez-Maqueda, A. Duran, and J.L. Pérez-Rodríguez, Appl. Clay Sci. 28[1-4] (2005) 245-255.
28. F.O. Aramide, O.D. Adepoju, and A.P. Popoola, J. Ceram. Process. Res. 19[6] (2018) 483-491.
29. C.J. Ngally Sabouang, J.A. Mbey, F. Hatert, and D. Njopwouo, J. Asian Ceram. Soc. 3[3] (2015) 360-367.
30. T. Iiyama, Proc. Jpn. Acad. 31[3] (1955) 166-168.
31. N.N. Sampathkumar, A.M. Umarji, and B.K. Chandrasekhar, Mater. Res. Bull. 30[9] (1995) 1107-1114.
32. F.A.C. Oliveira, N. Shohoji, J.C. Fernandes, and L.G. Rosa, Sol. Energy 78[3] (2005) 351-361.
33. S.L. Correia, K.A.S. Curto, D. Hotza, and A.M. Segadães, Mater. Sci. Forum 498-499 (2009) 447-452.
34. D. Wattanasiriwech, C. Sangtong, and S. Wattanasiriwech, ScienceAsia 33[1] (2007) 125-130.
35. S.Y.R. López and J.S. Rodríguez, AZoJomo, 4[July] (2008) 1-7.